Cell, Volume *127*

Supplemental Data

Substrate-Specific Translocational Attenuation during ER Stress Defines a Pre-Emptive Quality Control Pathway

Sang-Wook Kang, Neena S. Rane, Soo Jung Kim, Jennifer L. Garrison, Jack Taunton, and Ramanujan S. Hegde

Supplemental Notes

1. It is worth noting that the non-translocated species of PrP was not always readily visualized as in Fig. 1, even under conditions of stress when its generation was increased. This is apparently due to the rapid degradation of non-translocated PrP by a proteasome-dependent pathway (Drisaldi et al., 2003, Rane et al., 2004, and Fig. 3 and 4 of this study). Only when pulse-labeling times were minimized (less than ~15 min) and/or the proteasome was simultaneously inhibited during the experiment (e.g., Fig. 1B) was non-translocated PrP reliably observed. This is presumably the reason many previous studies of PrP have not noted this non-translocated population, and why our own experiments using longer pulse-labeling times (c.f., Fig. 2) or immunoblotting often show little or no cytosolic PrP.

2. The decrease in PrP glycosylation during acute stress (Fig. 1A) is compatible with several plausible explanations including: (i) decreased activity of the oligosaccharyl transferase; (ii) decreased access to sites of glycosylation on PrP due to its misfolding; (iii) increased retrotranslocation (and subsequent deglycosylation by cytosolic N-glycanase); (iv) selective degradation of membrane-bound PrP transcript (resulting in selective synthesis of non-targeted mRNA); (v) decreased translocation into the ER. All but the last two of these is effectively ruled out by the demonstration that signal sequence replacement restores glycosylation efficiency under the same stress conditions (Fig. 1B). While it is possible that the piece of mRNA encoded by the PrP signal sequence causes the effects observed, this seems unlikely given that substantial changes to the nucleic acid sequence (without altering the protein sequence) had no effect on stress-dependent changes in PrP biosynthesis (Fig. S2). Thus, the relatively circumscribed role of the signal sequence during the early stages of PrP biosynthesis limits the possible explanations to those involving targeting to the translocon and initiation of translocation. After these steps are completed, the signal sequence is co-translationally removed by signal peptidase by the time ~150 amino acids of PrP are synthesized (Kim and Hegde, 2002), well before the glycosylation sites (at positions 181 and 197) are even synthesized. From this point, the fate of PrP, Prl-PrP, and Opn-PrP are ostensibly equivalent in that they all are translocated into the same ER lumenal environment, encounter the same biosynthetic machinery, and subjected to the same quality control pathways. Although signal sequences can have functions after their removal, no evidence for such a role in PrP biosynthesis has emerged. Similarly, while the choice of signal sequence can influence PrP topology (Rutkowski et al., 2001; Ott and Lingappa, 2004), the alternate

topologic variants represent at most a few percent of the total PrP synthesized in vivo (Hegde et al., 1998a; Kim et al., 2002; Stewart and Harris, 2001). And finally, the examples where signal sequences influence glycosylation directly (Anjos et al., 2002; Rutkowski et al., 2003) are all cases of close juxtaposition of the signal sequence cleavage and glycosylation sites, which is not the case with PrP. Thus, the stress-dependent effect on PrP glycosylation must be due to an event influenced by the signal sequence, which in turn implies it occurs before ~150 amino acids of PrP are synthesized. Hence, the only plausible explanation is a co-translational attenuation of forward translocation into the ER. Based on several in vitro studies, this could be due to either a failure to successfully initiate translocation (Voigt et al., 1996; Fons et al., 2003) or co-translational slippage out of the translocon to the cytosol (Garcia et al., 1988; Ooi and Weiss, 1992; Nicchitta and Blobel, 1993; Hegde and Lingappa, 1996; Hegde et al., 1998b).

3. Although one might have expected the non-translocated glycoproteins generated during ER stress (e.g., Fig. 5C, 5E) or CT treatment (Fig. S7) to be visualized as extra bands in the cytosolic fraction, this is not the case for several reasons. First, most proteins aborted in their translocation have hydrophobic domains that do not allow them to be released efficiently into the soluble cytosolic fraction upon treatment of cells with low concentration of digitonin (e.g., Fig. S3 in the case of PrP). Second, the non-translocated material appears to be rapidly ubiquitinated (perhaps in some cases, co-translationally; Turner and Varshavsky, 2000) and degraded (e.g., Fig. 4A). And third, the relative abundance of radiolabeled cytosolic proteins versus ER-targeted glycoproteins is roughly 5:1, obscuring the detection of non-translocated ER proteins in total cytosolic fractions. Note however that upon immunoprecipitation, non-translocated proteins can indeed be detected in the cytosolic fraction (Fig. S3), albeit at relatively low yield even under conditions where translocation is inhibited completely with CT.

4. To gain insight into the step(s) at which translocation is attenuated during pQC and guide us in its reconstitution in vitro, we employed semi-permeabilized cells in which cytosolic mRNAs, ribosomes, and factors could be separated from membrane-bound components (see Fig. S10A). In this approach, semi-permeabilized cells lacking cytosolic contents are added to an in vitro translation reaction containing ^{35}S-Methionine to complete the translation (i.e., 'read-out') of endogenous mRNAs engaged by membrane-bound ribosomes. The disposition of the radiolabeled products (translocated into the ER or not) can then be assessed using a protease protection assay. Translocational attenuation at the membrane would result in mRNAs being recovered in the semi-permeabilized cells, but failure of their translated products to be successfully sequestered into the ER lumen. By contrast, a targeting defect of a protein would lead to the respective mRNA being cytosolic, therby being lost at the semi-permeabilization step itself. Hence, the protein product would not be generated upon readout of the semi-permeabilized cells. The semi-permeabilization, readout reaction, and ability to effectively remove mRNAs that fail to target to the ER were first tested in control experiments (Fig. S10B).

Upon applying this assay to acutely stressed cells, we observed the readout products from membrane-bound ribosomes to be reduced to ~65% of control cells (Fig. S10C, lanes 1-3). This decrease was uniform among the various proteins visualized by the readout assay (see quantitation of individual bands in Fig. S10D), presumably because translational attenuation prior to semi-permeabilization led to decreased amounts of engaged mRNAs. Upon protease digestion of the membrane-bound readout samples (Fig. S10C, lanes 4-6), we consistently found the degree of overall protection (which reflects translocation into the ER lumen) to be lower (by

~30-40%) for the stressed samples (Fig. S10E). Quantitation of individual bands on the autoradiograph (Fig. S10D) indicated that this overall decrease was an average of some proteins whose level of protection was substantially decreased in the stressed cells and others whose degree of protection was largely unaffected. This effect was even more obvious when the semi-permeabilized cells were re-isolated after protease digestion to remove proteolytic fragments generated from non-translocated products (Fig. S10F). Although some of these differences in protease sensitivity could be due to differences in membrane protein folding and not translocation, this seems unlikely due to the use of very high concentrations (500 μg/ml) of the highly active proteinase K. Thus, the stressed cells appear to show a substrate-specific decrease in translocation by this assay that mirrors results from the analysis of glycoprotein biogenesis in vivo.

Importantly, including a small amount of in vitro synthesized transcript for Prl in the translation reactions led to equal levels of Prl synthesis in stressed and unstressed samples (Fig. S10G). Furthermore, a portion of the exogenously translated Prl was translocated into the ER of the semi-permeabilized cells and subsequently protected from protease. Since Prl translocation and protease protection were equal in all three samples, we could rule out any differences in ER abundance or integrity as the explanation for different degrees and patterns of protease protected translation products in the stressed cells. Hence, although the profile of mRNAs that are targeted to the ER membrane during acute stress are similar (albeit reduced in overall amount) to unstressed conditions, the successful entry of the translated products into the protease-protected space of the ER lumen is diminished for a subset of these proteins. This suggests that the translocation defect in stressed cells that facilitates pQC is likely to be at a post-targeting step (i.e., after the mRNA has arrived at the ER membrane).

5. After solubilization, the reconstitution of proteins into the lumen of rRM to high concentrations has proven to be technically difficult. Unlike membrane proteins that become concentrated in the bilayer upon detergent removal, soluble proteins must rely on becoming trapped in the vesicle during its formation, therby limiting its concentration in the lumen to that present in the solution during reconstitution. Unfortunately, for reasons that are not entirely clear, very high total protein concentrations during the reconstitution procedure seem to interfere with vesicle assembly and recovery. This limits the maximal concentration of proteins achievable in the lumen of rRM to levels well below the normal concentration of lumenal contents (estimated to be at least 100 mg/ml).

6. Although we do not yet understand how changes on the lumenal side of the ER membrane can influence the function of signal sequences that operate largely on the cytosolic face of the ER, several models are plausible. Because lumenal chaperones can interact with translocating nascent proteins early in their synthesis, it is possible that for some substrates, lumenal protein interactions are important to prevent slippage out of the translocon. Such a model is consistent with observations of polypeptide slippage through the translocon (Garcia et al., 1988; Ooi and Weiss, 1992; Nicchitta and Blobel, 1993; Hegde and Lingappa, 1996; Hegde et al., 1998b), a possible gap between the membrane-bound ribosome and translocon (Menetret et al., 2005), and the apparently different affinities among signal sequences for the translocon (Kim et al., 2002). Thus, for some substrates, weakly interacting signals may allow slippage through the ribosome-translocon gap unless the mature domain of the polypeptide interacts with a lumenal chaperone immediately after its exposure to the lumen. Another model involves lumenal chaperones

altering the gating properties of the translocon such that some signals are influence in their ability to productively engage the translocation apparatus. Support for this model comes from the observation that BiP may influence or be part of the lumenal gate of a mammalian translocon (Hamman et al., 1998), and that the gating efficiencies of signal sequences varies among substrates (Kim et al., 2002). And finally, one of more lumenal components could influence the function of an accessory translocon factor (such as TRAM or the TRAP complex) that has already been shown to be required for translocation of selected substrates in a signal sequence-dependent manner (Voigt et al., 1996; Fons et al., 2003).

7. Although the magnitude of translocational attenuation (~30-50%) during acute stress is quite modest, two arguments can be made for its physiological relevance. First, evidence for the importance of even small changes in substrate burden during stress has been provided by recent studies on the role of translational attenuation in mice. Mice that are unable to attenuate translation during acute stress [due to a non-phosphorylatable eIF2α (S51A)] show a severe phenotype in highly secretory tissues (Scheuner et al., 2001). Remarkably however, even mice heterozygous for eIF2α(S51A), capable of at most half the level of translational attenuation compared to wild type mice, nonetheless show a diabetic phenotype ascribed to impaired β-cell function caused by exceeding the folding capability of the ER (Scheuner et al., 2005). Conversely, artificially attenuating translation by either PERK activation or by use of a translational inhibitor can be protective in cell culture models of ER stress and toxicity (Tan et al., 1998; Lu et al., 2004). Thus, in at least some cell types and under some conditions, the ER biosynthetic machinery is working at close to its capacity, making the reduction of substrate burden under stress conditions especially critical to cell viability. By adding a second layer of attenuation that is selective to the site of stress, translocational attenuation may permit the cell to maintain general translation at levels higher than it could otherwise afford. This would allow a higher level of synthesis of any essential non-ER proteins, whose folding and maturation are presumably not compromised during ER stress. The second reason a ~30-50% effect on overall translocation is likely to be significant is because not all substrates are affected uniformly. Especially problematic proteins (whose folding is particularly complex and/or highly dependent on multiple chaperones) may be attenuated to a greater degree than other proteins whose propensity to misfold is minimal. Thus, while the *average* attenuation is modest, the range appears to be broad and substrate-dependent. This may explain why bypassing pQC for a single (especially misfolding-prone) substrate such as PrP can have consequenes for a very general outcome like susceptibility to ER stress. Thus, the degree of translocational attenuation may be commensurate with the overall risk of terminal misfolding in the ER lumen. Similarly, proteins whose entry into the ER is important even during ER stress may not be subject to this type of regulation. Indeed, we have found that BiP (like TRAPα in Fig. 5F), whose upregulation is critical for recovery from and adaptation to stress, maintains a high level of translocation even during maximal acute stress (Fig. 7H).

Supplemental Experimental Procedures

Materials

Antibodies were described previously or from the following sources: TRAPα, Sec61β, and TRAM (Fons et al., 2003); 3F4 mouse monoclonal against PrP (Signet); VCAM1 (Santa Cruz Biotechnologies); GFP (Clontech); BiP (BD Biosciences); PDI and Cnx-N (StressGen). Expression constructs encoding PrP, Prl, Prl-PrP, PrP-Prl, Opn-PrP, PrP-GFP, Prl-PrP-GFP, and VCAM1, have been described (Kim et al., 2002; Fons et al., 2003; Rane et al., 2004; Garrison et al., 2005). The GFP expression construct was from Clontech. The coding regions of Frizzled-7, CRFR, and TRAPα were amplified by PCR and subcloned into a pCDNA3.1-based vector. Prl-CRFR and Opn-Prl were made using a strategy described previously for other signal sequence fusions (Kim et al., 2002). Frizzled-7, CRFR, and Prl-CRFR were each tagged at the C-terminus with an epitope (KTNMKHMAGAAA) recognized by the 3F4 antibody. PrP-mod was made by digesting the PrP expression plasmid with Bgl2 and PflM1 (which flank the signal sequence), and replacing the removed region with synthetic oligonucleotides coding for the sequence in Fig. S2A. Cotransin was prepared as described (Garrison et al., 2005) and dissolved in DMSO. DTT was from Roche and dissolved in water. Tg, Tm, BFA, MG132, and ALLN were from Calbiochem and dissolved in DMSO or EtOH (BFA). Each compound was first tested in preliminary experiments to determine the optimal concentration for each cell type. For BFA, efficacy was judged by dispersal of Golgi in live cells using a fluorescent protein-tagged marker (Mannosidase II; Sciaky et al., 1997). MG132 was used at either 5 μM or 10 μM, concentrations that lead to partial inhibition as judged by the level of cytosolic PrP accumulation (Rane et al., 2004). DTT and Tg were used at concentrations sufficient to induce translational attenuation (a proximal indicator of ER stress) to a level of ~30-70% (see Fig. S1). For HeLa cells, this was 10 mM and 10 μM, respectively. Tm was used at a concentration of 1 μg/ml. DeoxyBigCHAP and Digitonin were from Calbiochem. Digitonin was purified further as described (Gorlich and Rapoport, 1993). Immobilized ConA was from Amersham-Pharmacia and washed into IP buffer (see below) just before use for capture of glycoproteins.

Cell Culture

HeLa, Cos-7, and N2a cells were cultured in DMEM containing 10% FBS at 5% CO_2. HeLa cells were transfected with Effectene (Qiagen); N2a cells were transfected with Lipofectamine 2000 (Invitrogen). Stable cell lines were generated by selection in Zeocin for 4 weeks, followed by subcloning of individual colonies. Several individual clones at different expression levels were analyzed. Data are shown for two clones whose levels of expression and growth rates were the same. Replating viability assays were performed on cells in either 96-well dishes or 35 mm dishes. Following the treatments, cells were trypsinzed, collected, sedimented, and resuspended in fresh media. The total number of viable cells were counted in a hemocytometer using trypan blue. Equal numbers of cells for each condition (usually between 2,500 and 10,000) were plated into 10 cm dishes, and allowed to grow for between 8 and 10 days before fixation in methanol and staining with crystal violet. To quantify the results, the plates were digitized using a flatbed scanner, and a threshold function applied to convert images to black colonies on a white background. The total number of black pixels on each plate (which takes into account colony number and colony size) was measured and used to determine relative growth. It should be noted that all experiments shown in any panel were performed in parallel. Results from experiments performed on different days were not compared because of variations in growth and culture

conditions (note for example, the differences in colony size and number among different experiments). However, we confirmed in multiple independent experiments (at least three) that the *relative* differences shown in the figures were consistently observed. For the re-plating assays (Fig. 4C), treated cells from a 35 mm dish were trypsinized and replated with fresh media into 96-well plates which were allowed to grow for up to 72 h before harvesting and analysis by immunoblots. Immunofluorescence staining with 3F4 anti-PrP and confocal microscopy was as previously described (Rane et al., 2004).

Labeling and Biochemical Analyses of Cultured Cells

Pulse-labeling was performed on cells pre-incubated for 30 min in serum-free media lacking methionine and cysteine, to which Translabel (MP-Biomedical) was added at a concentration of 200 μCi/ml to initiate the labeling. Chase was carried out in complete media lacking label. Cells were harvested for immunoprecipitation in 1% SDS, 0.1 M Tris, pH 8, boiled, and diluted 10-fold in IP buffer (50 mM Hepes, pH 7.4, 100 mM NaCl, 1% Triton X-100) prior to addition of antibodies. Fractionation of cytosolic from non-cytosolic proteins using selective extraction with digitonin (Fig. S3A) was as before (Levine et al., 2005). Each fraction was subsequently immunoprecipitated using antibodies against GFP. Solubility assays for PrP were as described (Rane et al., 2004). Fractionation of cytosolic and glycoproteins (by the scheme shown in Fig. 5A) was performed on cells growing and labeled in 35 mm dishes. Cells were first washed in 1 ml PBS and extracted on ice with 1 ml KHM buffer (110 mM KAc, 20 mM Hepes, pH 7.2, 2 mM MgAc2) containing 150 ug/ml digitonin for 5 min. The cytosolic extract was reserved, and the remaining material was washed once in KHM and subsequently extracted in 1ml IP buffer to recover the non-cytosolic proteins. The glycoproteins were recovered from the non-cytosolic fraction by incubation for 1 h with 50 ul packed ConA beads, followed by washing 3 times in IP buffer, and elution for 1 h at room temperature in 350 ul IP buffer containing 0.25 M α-methyl-D-mannopyranoside. Aliquots of the cytosolic extract and eluted glycoproteins were analyzed directly on SDS-PAGE and autoradiography. Quantification of radiolabeled products utilized a Typhoon phosphorimager and accompanying software (Molecular Dynamics). All gels were also stained with coomassie blue to confirm equal recovery and loading of total proteins, glycoproteins, and IgG (in the case of immunoprecipitations). Any experiments where recovery was not uniform for all samples were not analyzed. This ensured that any differences in radiolabeled products were not a consequence of technical variability.

Analysis and Modulation of Chaperones in Cultured Cells

For biochemical analysis of chaperones, cells in 35 dishes were treated as indicated in the legend to Fig. 7, transferred to ice, and pre-extracted with KHM containing 150 μg/ml digitonin and 10 U/ml apyrase for 5 min followed by a wash in KHM containing 10 U/ml apyrase. This led to removal of cytosolic contents and depletion of ATP levels. The remaining cellular material was then solubilized by scraping into 250 ul of 50 mM Hepes, pH 7.4, 100 mM NaCl, 2 mM MgCl2, 0.5% Triton X-100. The lysate was centrifuged for 5 min at 10,000 rpm in a microcentrifuge and the supernatant removed as the ‘soluble’ fraction. The pellet was dissolved in SDS-PAGE sample buffer and referred to as the ‘insoluble’ fraction. The soluble fraction was either analyzed directly in some cases or 200 ul of it was applied to a 2ml linear 5%-25% sucrose gradient prepared in the Triton X-100 lysis buffer above. After centrifugation for 3 h at 55,000 rpm in a TLS-55 rotor (Beckman), 200 ul fractions were collected from the top and analyzed by SDS-PAGE and immunoblotting as indicated in the Figure legends. For pre-conditioning, cells were

treated with 10 mM DTT for 1 h followed by replacement with fresh media and recovery for 16 h.

In Vitro Translation and Readout Analyses

Readout assays on semi-permeabilized cells (Fig. S10) were carried out on cells grown in 35 mm dishes. The cells were placed on ice, semi-permeabilized with 100 ug/ml digitonin in KHM for 5 min, and the digitonin extract removed. The cells remaining on the dish were rinsed once in KHM buffer, scraped into 2 ml KHM, isolated by sedimentation for 2 min at 1000 rpm in a microcentrifuge, and resuspended in 10 ul KHM. The semi-permeabilized cells were used immediately (at a concentration of 2.6 ul per 25 ul total reaction volume) in translation reactions containing rabbit reticulocyte lysate. Translations were for 30 min at 32°C. Where indicated, in vitro synthesized transcripts coding for control proteins were included in the translation reaction. Translation reactions were divided into two aliquots on ice, one of which was digested with proteinase K (PK) at 0.5 mg/ml for 1 h. The reactions were terminated with 5 mM PMSF and transferred directly to 10 volumes of boiling 1% SDS, 0.1 M Tris, pH 8. Alternatively (Sup. Fig. S10F), the protease-digested cells were re-isolated by centrifugation and dissolved directly in SDS-PAGE sample buffer. To analyze cytosolic ribosomes (Supl. Fig. S10F), the cytosolic extract after digitonin treatment was centrifuged at 70,000 rpm for 30 min in a TLA100.3 rotor and the mRNA-bound ribosomal pellet was resuspended in 10 ul KHM. This was added to translation reactions as above. Quantification of the radiolabeled products utilized a phosphorimager.

Membrane Fractionation and Reconstitution

RM were prepared as described (Walter and Blobel, 1983). LD-RM were prepared as described in Garrison et al., 2005: 100 ul RM at a concentration of 1 eq/ul in membrane buffer (50 mM Hepes, pH 7.4, 250 mM sucrose, 1 mM DTT), were diluted with four volumes of membrane buffer containing 0.075 % DeoxyBigCHAP on ice. After 10 min on ice, the microsomes were sedimented at 100,000 rpm for 15 min at 4°C in a TL100.3 rotor. The supernatant was removed, and the tube was carefully rinsed (without disturbing the pellet) twice with 500 ul of membrane buffer (lacking detergent). The pellet was resuspended in 500 ul of the membrane buffer (lacking detergent), transferred to new tubes, and sedimented again as above. After removing the supernatant, the membranes were resuspended in 100 ul. mRM were prepared exactly as above and in parallel, but without detergent in any of the buffers. Serial dilutions of mRM and LD-RM were analyzed on a single gel and immunoblotted with BiP and PDI to estimate the degree of lumenal protein depletion, which proved to be ~80-90%. To prepare rRM, we used the method described in Fons et al., 2003: RM (at a concentration of 1 eq/ul in membrane buffer) were first pre-extracted by dilution with an equal volume of membrane buffer containing 2% saponin. After 5 min on ice, the membranes were isolated by sedimentation (100,000 rpm for 15 min at 4°C in a TL100.3 rotor) and resuspended in extraction buffer (350 mM KAc, 50 mM Hepes, 5 mM MgAc2, 15% glycerol) in the original volume. After addition of DeoxyBigCHAP to 0.8% and incubation on ice for 10 min, the insoluble material was removed by centrifugation (100,000 rpm for 30 min at 4°C in a TL100.3 rotor), and the detergent extract reconstituted into proteoliposomes by detergent removal as previously described (Fons et al., 2003). The pre-extraction step above removes ~90% of lumenal proteins, while the reconstitution and re-isolation procedure removes essentially any remaining lumenal proteins. We estimated rRMs to contain less than 2% of lumenal contents relative to RM. To reconstitute rRM with lumenal

proteins (Hegde et al., 1998b), a lumenal protein extract was prepared by extracting RM (at 1 eq/ul in membrane buffer) with an equal volume of 0.25% Digitonin in membrane buffer. After removing the membranes, the lumenal protein fraction was precipitated by adjusting the sample to 13% PEG-6000. The protein precipitate was collected by centrifugation in a microcentrifuge, and dissolved in extraction buffer in one-twentieth the original volume of starting RM. For co-reconstitution, this concentrated lumenal protein fraction was added in varying amounts to the membrane protein extract above and reconstituted into proteoliposomes by detergent removal as before (Fons et al., 2003). In vitro translation and translocation assays and determination of translocation by protease protection were performed as described previously (Fons et al., 2003).

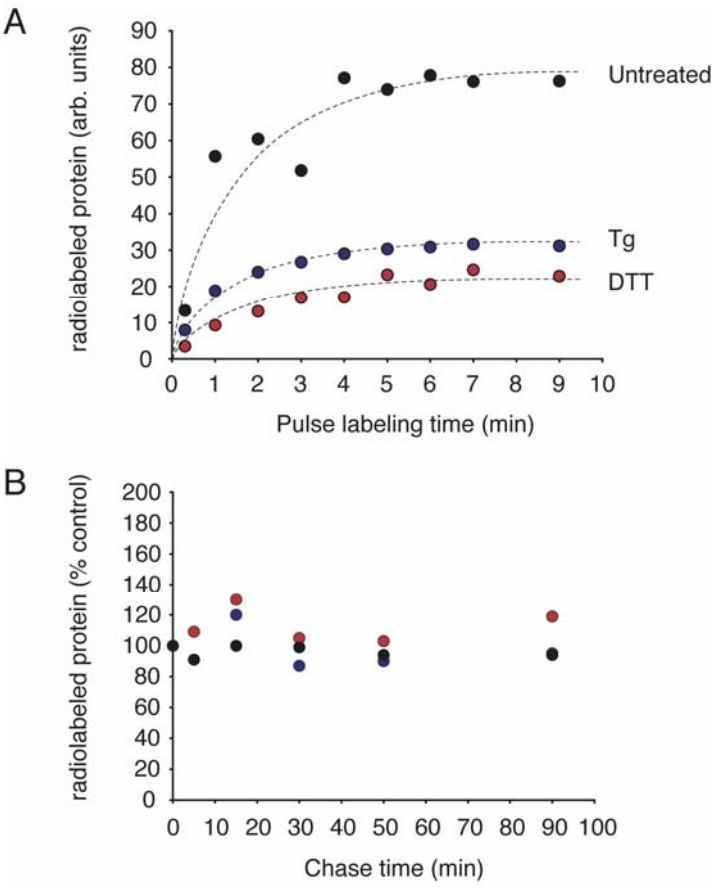

Figure S1. Relative Rates of Protein Synthesis and Degradation during Acute ER Stress

(A) Cultured Hela cells in 96-well dishes were pulse-labeled with [35]S-Methionine for the indicated times before quantification of total radiolabeled proteins by SDS-PAGE and phosphorimaging. Cells contained either no stressor (black symbols), Tg (blue symbols), or DTT (red symbols) during the entire experiment. The saturation of labeled protein after ~5 min in this experiment raised the possibility that non-linear kinetics of labeling could influence the quantification of some experiments. However, this concern can be mitigated by three observations. First, we have done experiments in which the labeling was for only 5 min and observe the same results as with longer labeling times (data not shown). Second, when using larger culture dishes (as is the case in nearly all experiments shown in the main text), incorporation of label was confirmed to be linear for at least 30 min (suggesting that this saturation effect may be due to the 96-well plate format). And third, even in experiments where incorporation is non-linear, the same kinetics are observed for both untreated and stressed cells, making it very unlikely that differences between them can be explained by the labeling alone.

(B) After pulse-labeling Hela cells in 96-well plates for 10 min as in panel A, the labeling media was replaced with unlabeled media and chased for the indicated times before quantitative analysis of total radiolabeled protein by SDS-PAGE and phosphorimaging. The data are normalized to the amount of radiolabeled protein present immediately after the pulse labeling (defined as time 0). Cells contained either no stressor (black symbols), Tg (blue symbols), or DTT (red symbols) during the entire experiment.

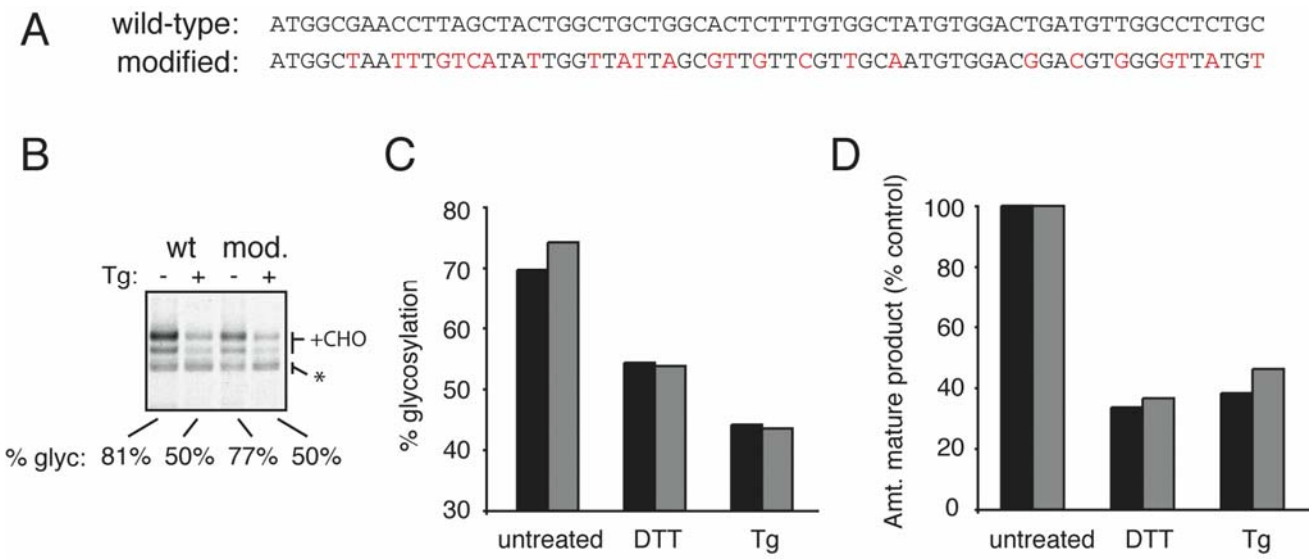

Figure S2. Effect of Nucleotide Changes in the Signal Sequence on PrP Biosynthesis

(A) Nucleotide sequences of the wild type PrP signal sequence and a modified version coding for the same protein sequence. Differences are indicated in red.

(B) The wild type and modified versions of PrP were analyzed for stress-dependent effects on their biosynthesis as in Fig. 1A. Note that in both cases, Tg stress causes a significant and comparable reduction in translocation as judged by decreased glycosylation. The positions of the glycosylated ('+CHO') and non-glycysylated ('*') species are indicated. A similar effect was observed with DTT stress (not shown).

(C) The degree of stress-dependent reduction in PrP glycosylation is plotted for the wild type (black bars) and modified (grey bars) versions of PrP.

(D) The reduction in generation of fully glycosylated mature PrP during acute stress was quantified as in Fig. 1A and normalized for the degree of overall translational attenuation. Note that during acute stress, the generation of fully glycosylated PrP is reduced to ~40% of what could be expected on the basis of translational attenuation alone. This effect was similar for both wild type PrP (black bars) and modified PrP (grey bars), suggesting that it is not influenced by changes in the nucleotide sequence of the signal sequence.

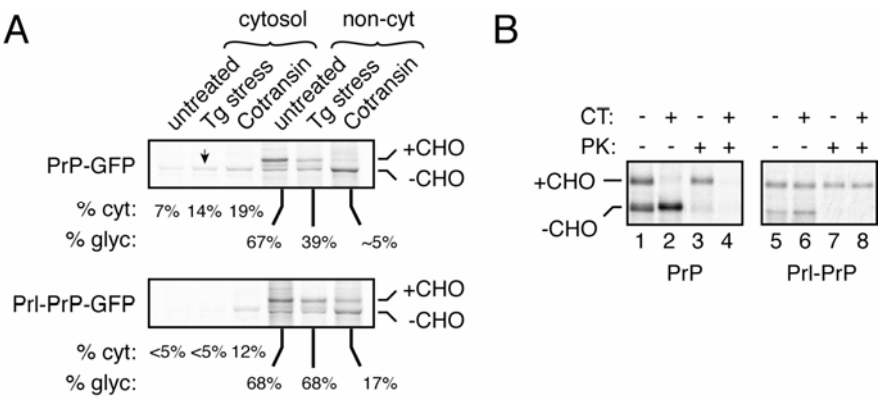

Figure S3. Analysis of PrP Translocation by Cell Fractionation

Cell fractionation experiments to directly demonstrate the cytosolic disposition of non-glycosylated PrP were confounded by its relative insolubility and propensity to aggregate (Ma and Lindquist, 2002; Drisaldi et al., 2003; Rane et al., 2004; Grenier et al., 2006). However, a GFP-tagged version of PrP (PrP-GFP) proved somewhat more amenable to fractionation and displayed the same selective reduction in translocation (as judged by decreased glycosylation) during acute ER stress as untagged PrP (panel A). At least a portion of unglycosylated PrP-GFP could now be observed in the cytosolic fraction, and this species increased (~ 2-fold) during acute stress (arrowhead, panel A). Importantly, the translocation efficiency of Prl-PrP-GFP was not changed significantly during stress, and it was not observed in the cytosolic fraction under either normal or stressed conditions (Panel A). Direct inhibition of PrP-GFP translocation with the translocational inhibitor Cotransin (CT; Garrison et al., 2005; see panel B) resulted in no translocation of PrP-GFP (and reduced translocation of Prl-PrP at this concentration in vivo), and increased amounts recovered in the cytosolic fraction. Note however that even when translocation is completely inhibited, only ~20-30% of PrP-GFP could be recovered in a soluble state in the cytosol, probably because the uncleaved hydrophobic domains at the N- and C-terminus of PrP-GFP complicate its efficient fractionation (Rane et al., 2004; our unpublished observations). This technical limitation notwithstanding, these results provide direct corroboration that PrP translocation is selectively reduced during acute ER stress in a signal sequence-dependent manner.

(A) The biosynthesis of PrP-GFP and Prl-PrP-GFP was analyzed by immunoprecipitation of pulse-labeled (30 min) and fractionated HeLa cells acutely treated with 10 μM Tg or 10 mM Cotransin for 30 min. The percent of total synthesized product that is in the cytosolic fraction ('% cyt') or glycosylated ('% glyc') is indicated. Glycosylated ('+CHO') and non-glycosylated ('-CHO') bands are indicated.

(B) PrP and Prl-PrP were translated and translocated in vitro using rough microsomal membranes in the presence or absence of 10 μM CT. Translocation of the products was assessed by a protease protection assay using proteinase K (PK). The unglycosylated ('-CHO') and glycosylated ('+CHO') forms are indicated. Note that CT inhibits translocation of PrP more potently than Prl-PrP, as evidenced by the lack of PrP glycosylation (lane 2) and protease protection (lane 4) in the presence of CT. At higher concentrations, some inhibition of Prl-PrP was observed. Since CT is more potent in vivo than in vitro (Garrison et al., 2005), this partial effect on Prl-PrP was easier to observe in some experiments than others (e.g., as in panel A above).

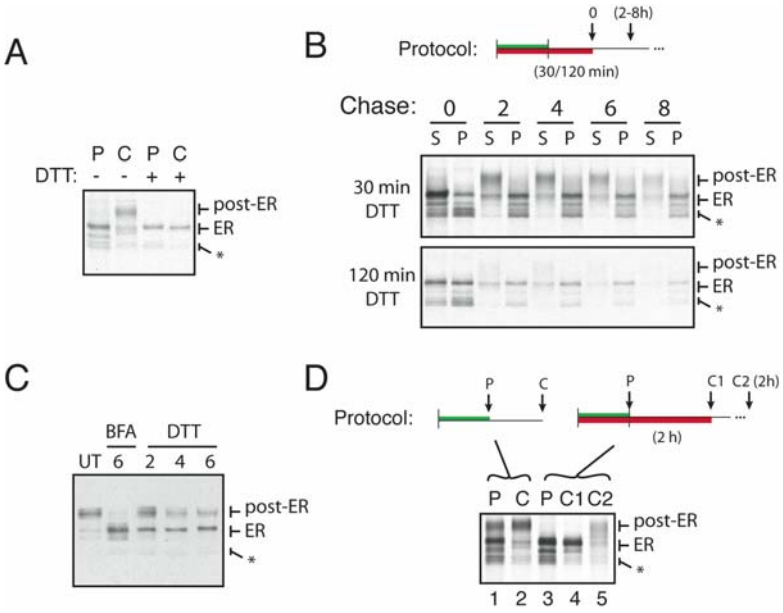

Figure S4. Analysis of PrP Trafficking during DTT and Brefeldin A (BFA) Treatment

(A) Cells transiently transfected with PrP were pulse labeled for 15 min ('P') and chased ('C') in the absence of label for 1 h. The entire pulse-chase was performed in the presence or absence of DTT. Unglycosylated ('*'), core-glycosylated ('ER'), and complex glycosylated ('post-ER') forms of PrP are indicated. Note that PrP, which contains two cysteines that need to be disulfide bonded to fold properly, is retained in the ER in the presence of ongoing DTT stress.

(B) Cells pulse-labeled for 30 min (green bar) were maintained in DTT (red bar) for 30 or 120 additional minutes before return to normal medium and collection of chase time points from 0 to 8h. Each sample was analyzed by solubility assays, immunoprecipitation, and autoradiography as in Figure 2A.

(C) Cells expressing PrP were treated with either DTT or BFA for up to 6 h before analysis by immunoblots. Note the accumulation of the ER form of PrP when ER-to-Golgi trafficking is prevented by BFA. The same form accumulates with DTT, albeit to a lesser extent due to translational and translocational attenuation during this time period.

(D) Cells were pulse-labeled for 30 min in the presence of BFA (lane 3), chased for 2 h without label (but in the presence of BFA; lane 4), and chased an additional 2 h after removal of BFA (lane 5). A pulse-chase in the absence of BFA is shown for comparison (lanes 1, 2). A schematic of the experiment is shown above the autoradiograph, with the period of labeling indicated in green and the period of BFA treatment indicated in red. Unglycosylated ('*'), core-glycosylated ('ER'), and complex glycosylated ('post-ER') forms of PrP are indicated. Note that even after being held in the ER for two hours with BFA, PrP is capable of trafficking to post-ER compartments. The incomplete maturation of its glycans is likely a consequence of trafficking through the Golgi simultaneously with Golgi re-assembly upon BFA removal.

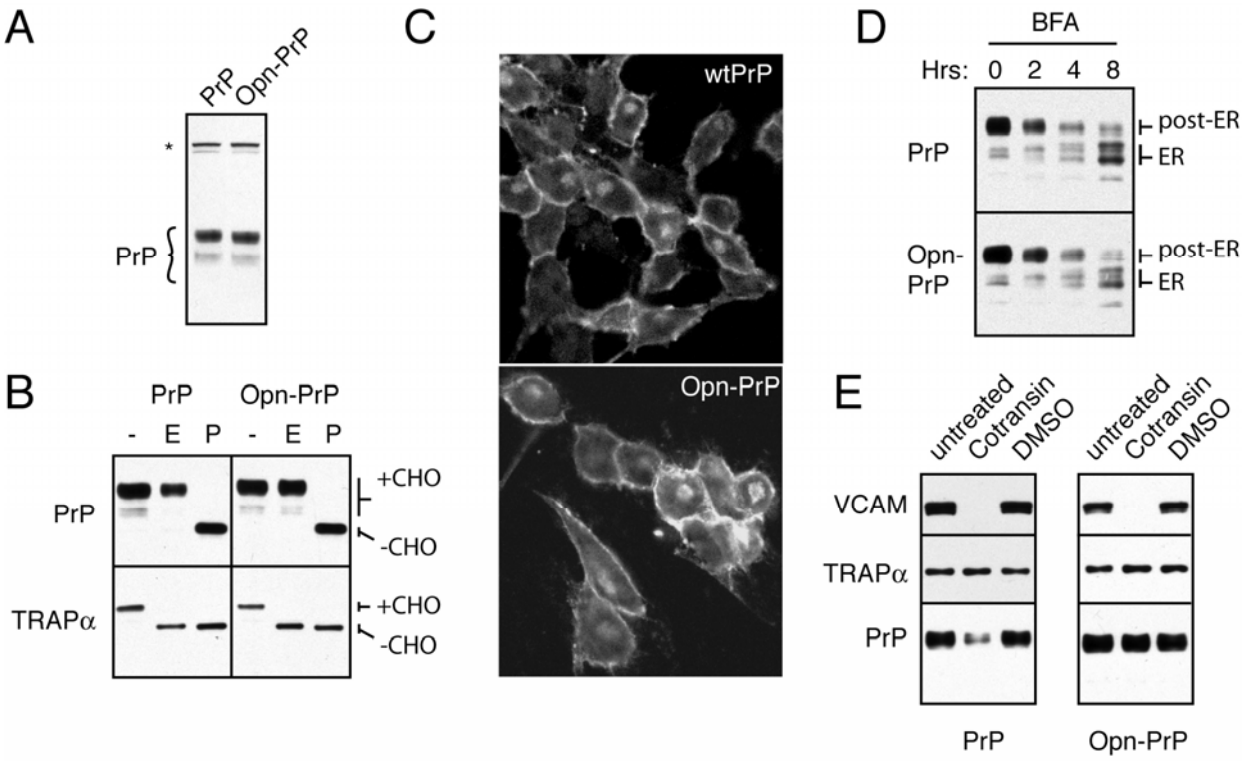

Figure S5. Characterization of PrP and Opn-PrP Cell Lines

(A) Immunoblot of expression levels in stable PrP and Opn-PrP cells. The background band ('*') serves as a loading control.

(B) Lysates from PrP and Opn-PrP cells were treated with Endoglycosidase H ('E') or PNGase F ('P') before immunoblotting for PrP and the resident ER glycoprotein TRAPa. The positions of glycosylated ('+CHO') and unglycosylated ('-CHO') species are indicated.

(C) Immunofluorescence detection of PrP and Opn-PrP in the respective stable cell lines.

(D) Cells stably expressing PrP or Opn-PrP were treated with BFA for the indicated times before analysis by immunoblot. The ER-retained forms of PrP accumulate at the same rate for PrP and Opn-PrP, indicating that in the absence of acute ER stress, the translocation efficiency of both proteins is essentially indistinguishable. Also note that BFA treatment leads to a variable degree of heterogeneity of the PrP glycoforms that accumulate in the ER over time, presumably due to the mixing of Golgi enzymes with the ER compartment.

(E) Cells stably expressing either PrP or Opn-PrP were transiently transfected with a VCAM1 expression plasmid and treated with CT (5 μM) for 8 h before analysis by immunoblots. PrP is inhibited by CT, while Opn-PrP is largely resistant to inhibition at this concentration. VCAM1 is inhibited equally in both cell lines, demonstrating that the resistance of Opn-PrP to CT is due to the signal sequence, and not an inherently resistant cell line. Opn-PrP was inhibited to a greater extent at higher concentrations of CT (~50% inhibition at 20 μM; data not shown).

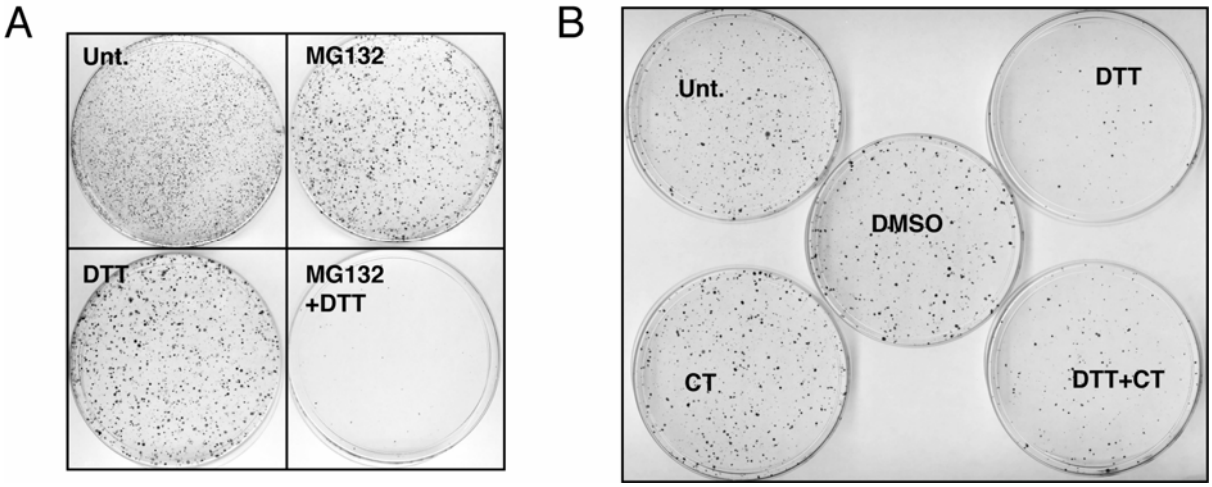

Figure S6. Colony Formation Assays for Cell Survival under Various Conditions

(A) PrP-expressing cells treated with DTT, MG132, or both agents for 18 h were re-plated in normal media and visualized 8 d later by staining with crystal violet.

(B) Opn-PrP expressing cells were treated with the indicated agents for 6 h before re-plating in normal media and visualization 8 d later by staining with crystal violet.

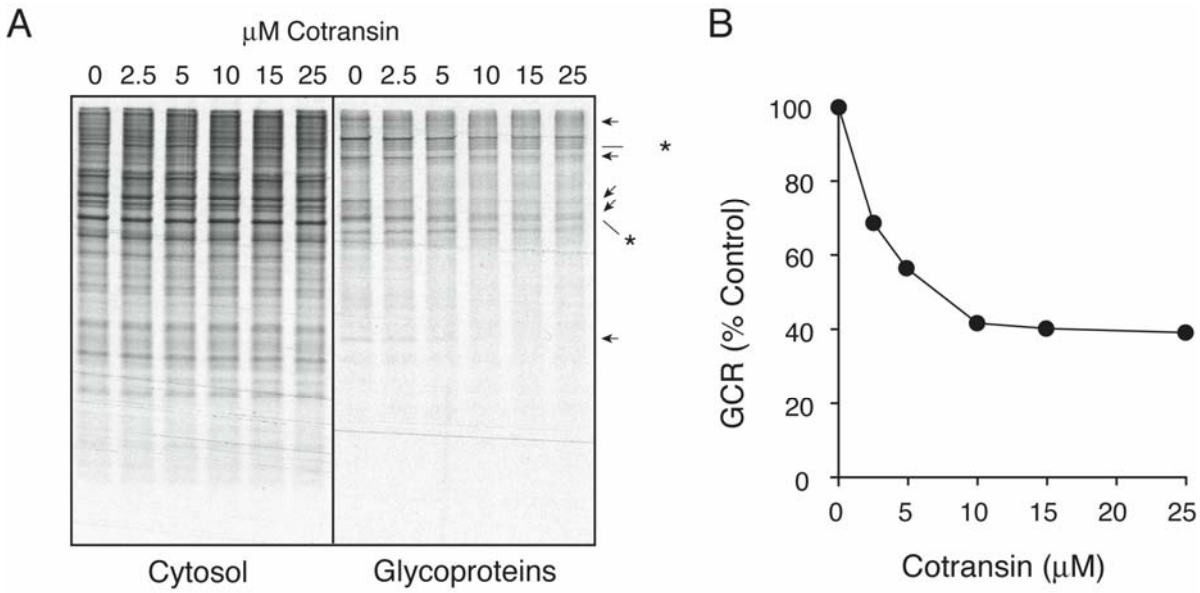

Figure S7. Characterization of Assay for Translocational Attenuation

(A) Cells pulse-labeled for 30 min with increasing concentrations of CT were separated into cytosolic and glycoprotein fractions and analyzed by autoradiography. Note that the glycoprotein samples are from a longer exposure of the film than cytosolic samples. The arrows point to bands that are reduced to varying degrees by CT (presumably due to inhibition of their translocation), while asterisks indicate bands that are largely refractory to CT. Note that no cytosolic proteins are affected by CT. Also, glycoproteins inhibited in their translocation by CT are not easily visualized in the cytosolic fraction for various reasons that are discused in Sup. Note 3.

(B) Ratio of total radiolabeled glycoprotein to cytosolic protein ratio (GCR) quantified from panel A, with the value from untreated cells arbitrarily set to 100%.

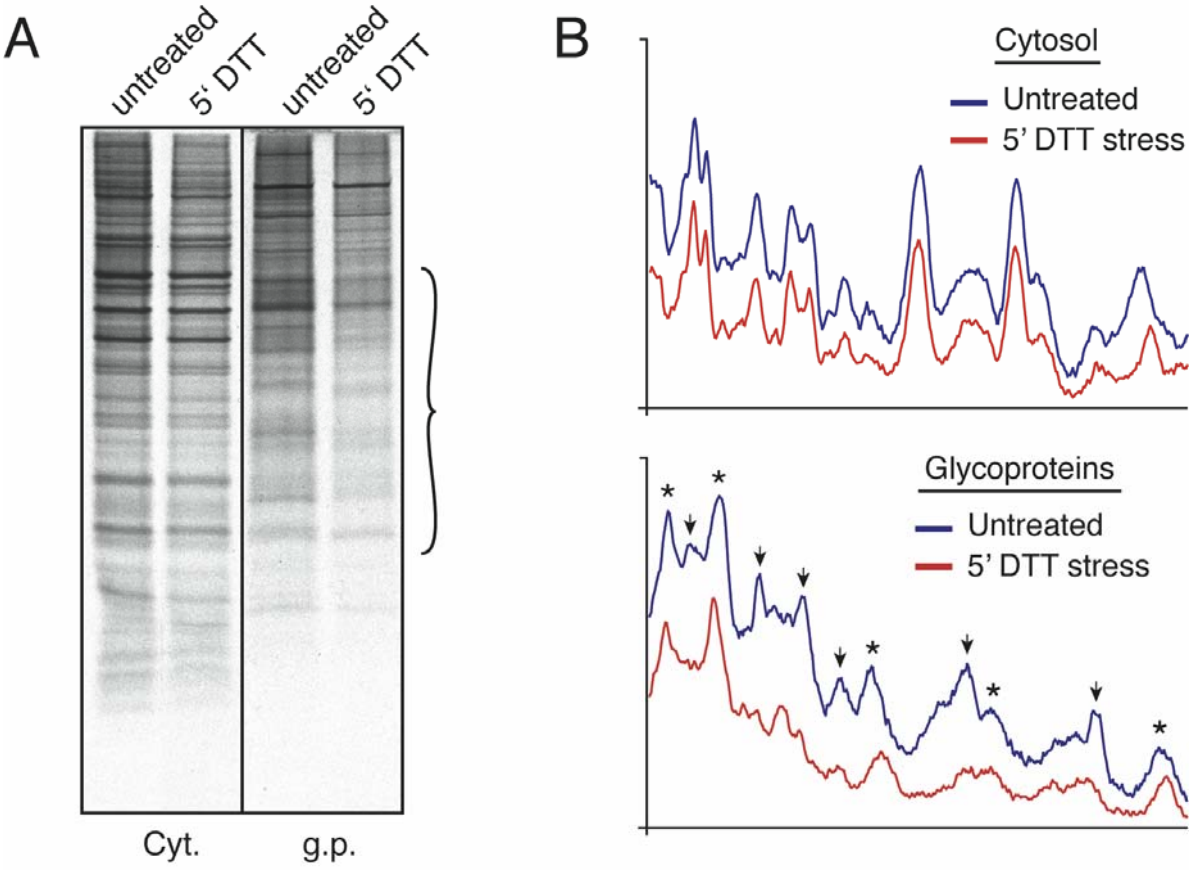

Figure S8. Profiles of Cytosolic Proteins and Glycoproteins during Acute ER Stress

(A) Cultured cells were left untreated or treated for 5 min with 10 mM DTT before pulse-labeling for 5 min and fractionation into cytosolic proteins and glycoproteins. The autoradiograph of newly synthesized cytosolic proteins and glycoproteins is shown at left. The region indicated by the bracket was analyzed by densitometry in panel B.

(B) Densitometry profiles from ~60 kD (left) to ~25 kD (right) of radiolabeled cytosolic proteins (top graph) and glycoproteins (bottom graph) from untreated and DTT-treated cells from panel A. Note that cytosolic proteins uniformly decrease during DTT treatment (due to translational attenuation), while the glycoproteins are reduced to variable levels. Arrows indicate bands that decrease substantially more than that attributable to translational attenuation, while asterisks indicate bands whose decrease is comparable to the level of translational attenuation. It should be noted that some of the changes to the profile of bands could be due to alterations in glycosylation efficiencies at some consensus sites in the presence of 10 mM DTT. However, the overall decrease in glycoproteins is not likely to be due solely to such an effect because a similar decrease was also observed in the presence of Tg (e.g., Fig. 5D), and because this effect was largely reversible depsite the presence of 10 mM DTT in cells preconditioned with an earlier stress (see Fig. 7F).

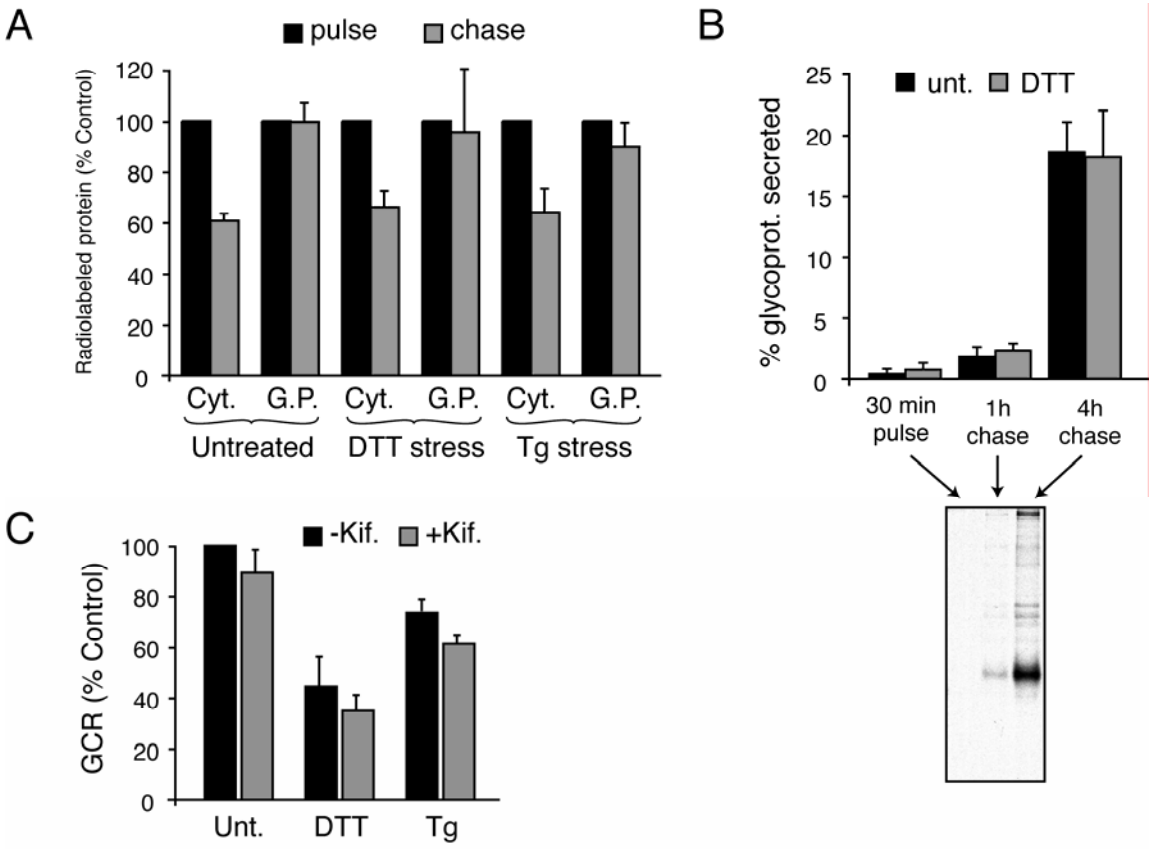

Figure S9. Decreased GCR during Acute ER Stress Is Not Due to Increased Degradation

(A) Total radiolabeled cytosolic proteins and glycoproteins were quantified after pulse-labeling (15 min) and chase in unlabeled media (1 h). Each chase value was normalized to its respective pulse value. Cells were either untreated, exposed to DTT, or exposed to Tg during the entire pulse and chase. The mean ± SD for three replicates is shown. Note that regardless of the treatment condition, ~40% of cytosolic proteins are degraded during the 1 h chase, while very little glycoproteins are lost to either degradation or secretion (see panel B).

(B) Cells were subjected to a 30 min pulse label followed by chase in unlabeled media for either 1h or 4h. The pulse-chase was performed on either untreated (black bars) or DTT-treated cells (grey bars). The radiolabeled glycoproteins in the cell lysate and media were captured by Con A, analyzed by SDS-PAGE, and quantified by phosphorimaging. The percent of radiolabeled glycoproteins secreted into the media is plotted (mean ± SD for three replicates), with a representative autoradiograph for the untreated samples shown below the graph. Note that less than 3% of synthesized glycoproteins are secreted into the media in the first hour.

(C) GCR from untreated or acutely stressed (30 min) cells was determined in the presence or absence of Kifunensine to inhibit access of glycoproteins to the ER-associated degradation (ERAD) pathway. The mean ± SD for three replicates is shown. Note that the GCR decrease during acute stress is the same in the presence or absence of Kifunensine, suggesting that increased ERAD is not involved in changes to the GCR.

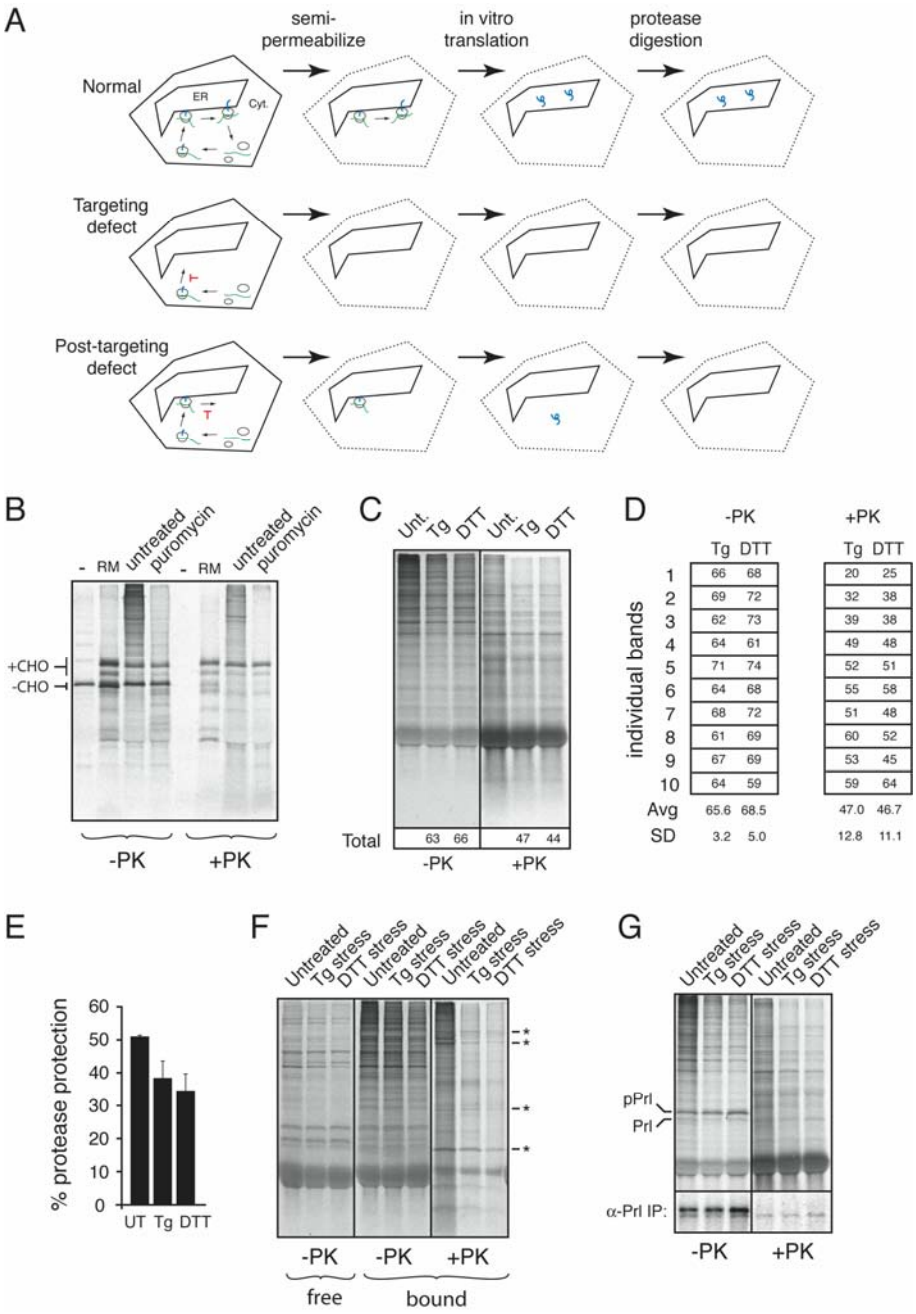

Figure S10. A Posttargeting Step Is Involved in Translocational Attenuation

(A) Experimental design of an assay to distinguish targeting from post-targeting mechanisms of translocational attenuation. Cultured cells are semi-permeabilized with digitonin to remove cytosolic contents including free ribosomes, and the permeabilized cells added to an in vitro translation reaction containing [35]S-Methionine to complete the translation (i.e., 'read-out') of mRNAs engaged by membrane-bound ribosomes. The location of these radiolabeled readout products is assessed by a protease protection assay. A defect in targeting or translation in the cells would manifest as a loss of membrane bound mRNAs, resulting in reduced or no readout products. By contrast, a defect at the level of translocation would permit recovery of membrane-bound mRNAs and their subsequent translation, but result in their accessibility to protease digestion.

(B) In vitro translation reactions containing transcript for PrP was carried out in the presence of: no additions ('-'), pancreatic rough microsomes ('RM'), semi-permeabilized cells ('untreated'), or cells pre-treated with puromycin (200 uM for 15 min) prior to semi-permeabilization ('puromycin'). Note that PrP is synthesized at comparable levels in all reactions. In the presence of either RM or semi-permeabilized cells, PrP is translocated into the ER lumen, as judged by its glycosylation ('+CHO') and protection from proteinase K (PK) digestion. In the untreated semi-permeabilized cells, numerous readout products are generated, which are protected to varying degrees from PK digestion. By contrast, the puromycin-pretreated semi-permeabilized cells generate substantially less readout products due to the loss of membrane-bound mRNAs under these conditions (see panel A).

(C) Cells treated as indicated were semi-permeabilized and the mRNAs engaged by membrane-bound ribosomes were allowed to complete synthesis in vitro. The samples were then subjected to proteinase K (PK) digestion and an aliquot of the total radiolabeled products before and after PK were visualized by autoradiography. The total radiolabeled products in the Tg and DTT lanes were quantified (% relative to untreated lane) and indicated below the respective lanes.

(D) Individual bands in the Tg and DTT lanes (arbitrarily denoted "1" through "10") were quantified (% relative to the same band in the untreated lane) and shown in the table. The average (Avg) and SD of the ten bands are also shown. Note that the level of reduced synthesis (in the -PK lanes) is very similar for all bands, while the degree of protease protection is substantially more variable from band to band (as indicated by the larger SD).

(E) The overall degree of protease protection (of all readout products) from four independent experiments as in panel C were tabulated (mean ± SD).

(F) Readout reactions were performed using semi-permeabilized cells that were pre-treated (before permeabilization) with either nothing ('untreated'), Tg, or DTT for 30 min. After PK digestion, the cells were re-isolated by sedimentation to remove proteolytic fragments. Note that with Tg or DTT, many products are not protected from PK digestion as efficiently as in untreated cells, indicative of their reduced translocation efficiency. The asterisks identify several proteins whose protection is not significantly affected by DTT or Tg, and hence appear to be constitutively translocated at the same efficiency as in untreated cells. In addition, non-membrane-bound (i.e., 'free') ribosomes isolated from the cytosolic extract generated by semi-permeabilization was also subjected to readout analysis. Note that the amount of radiolabeled readout products is reduced to comparable degrees with Tg and DTT for both the free and membrane-bound reactions, indicating that translational attenuation affects both populations uniformly.

(G) A readout reaction exactly as in panel D was performed in the presence of an in vitro generated transcript coding for Prl. The position of the precursor (pPrl) and processed forms of Prl are indicated. An aliquot of the samples was subjected to immunoprecipitation with anti-Prl antisera and the products are shown in the bottom panel. Note the equal levels of Prl synthesis, processing, and protease-protection in all three samples.

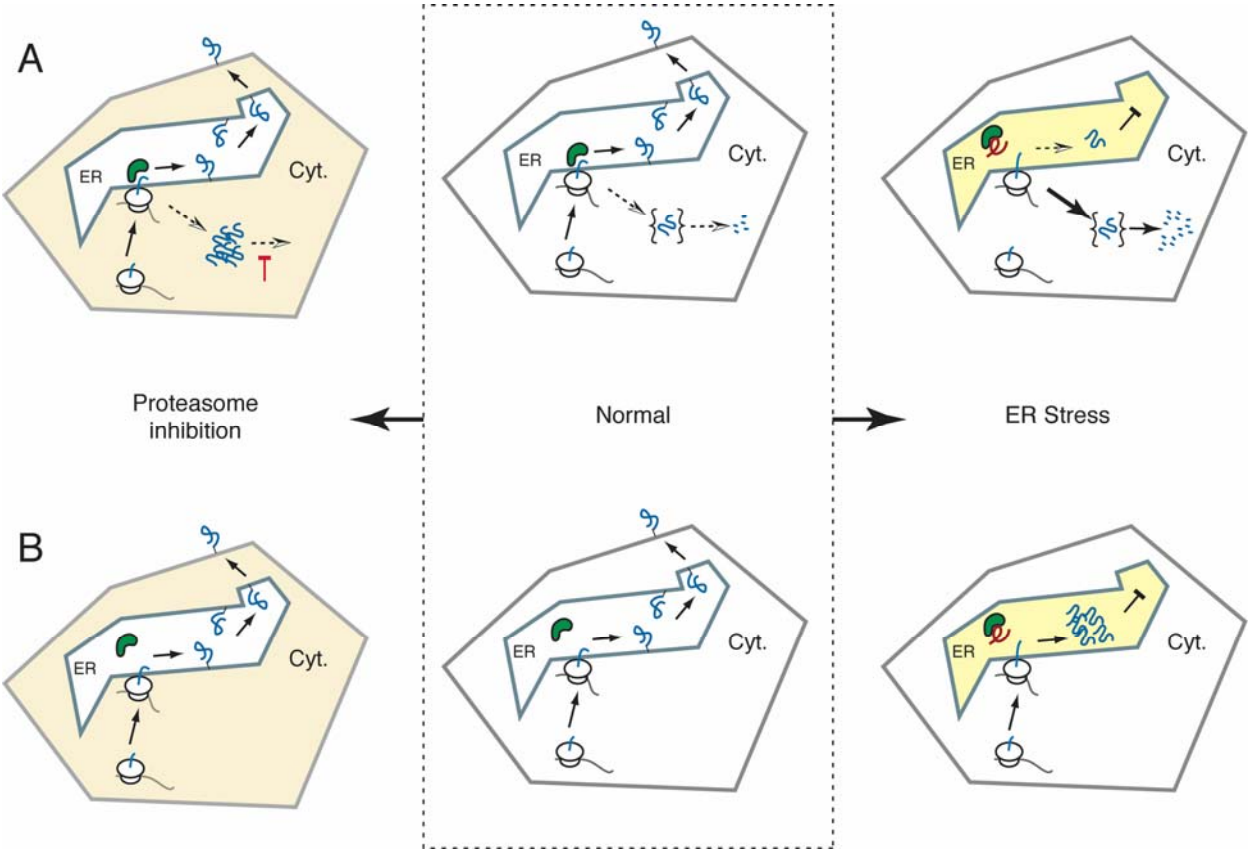

Figure S11. The Role of Translocational Attenuation in Protection from ER Stress

A translocationally attenuatable substrate (such as PrP) versus a constitutively translocated version (such as Opn-PrP) are shown in panels A and B, respectively. The center diagrams show normal targeting, maturation, and traffic to the cell surface for both substrates, with PrP translocation being at least partially dependent on the availability of yet unidentified lumenal factor(s) (e.g., BiP) indicated in green. Although not ordinarily detectable, a small fraction of PrP is not translocated due to signal sequence inefficiency and is rapidly degraded via a transient intermediate (indicated in braces). Under conditions of ER stress (right diagrams), the availability of the putative lumenal factor is reduced due to its association with misfolded proteins (indicated in red). This causes the translocation of PrP to be reduced, leading to a greater proportion of it being degraded in the cytosol. By contrast, translocation of Opn-PrP continues with high efficiency during ER stress, leading to the accumulation of misfolded, aggregation-prone protein in the ER lumen. The left diagrams show the consequenes of partial proteasome inhibition, which may occur during aging or the course of certain neurodegenerative diseases (Gray et al., 2003; Ciechanover and Brundin, 2003). Under these conditions, PrP, due to its slightly inefficient translocation, generates cytosolic aggregates that are not formed with Opn-PrP.

Supplemental References

Anjos, S., Nguyen, A., Ounissi-Benkalha, H., Tessier, M. C., and Polychronakos, C. (2002). A common autoimmunity predisposing signal peptide variant of the cytotoxic T-lymphocyte antigen 4 results in inefficient glycosylation of the susceptibility allele. J Biol Chem 277, 46478-46486.

Ciechanover, A., and Brundin, P. (2003). The ubiquitin proteasome system in neurodegenerative diseases: sometimes the chicken, sometimes the egg. Neuron 40, 427-446.

Drisaldi, B., Stewart, R. S., Adles, C., Stewart, L. R., Quaglio, E., Biasini, E., Fioriti, L., Chiesa, R., and Harris, D. A. (2003). Mutant PrP is delayed in its exit from the endoplasmic reticulum, but neither wild-type nor mutant PrP undergoes retrotranslocation prior to proteasomal degradation. J Biol Chem 278, 21732-21743. Epub 22003 Mar 21726.

Fons, R. D., Bogert, B. A., and Hegde, R. S. (2003). Substrate-specific function of the translocon-associated protein complex during translocation across the ER membrane. J Cell Biol 160, 529-539.

Garcia, P. D., Ou, J. H., Rutter, W. J., and Walter, P. (1988). Targeting of the hepatitis B virus precore protein to the endoplasmic reticulum membrane: after signal peptide cleavage translocation can be aborted and the product released into the cytoplasm. J Cell Biol 106, 1093-1104.

Garrison, J. L., Kunkel, E. J., Hegde, R. S., and Taunton, J. (2005). A substrate-specific inhibitor of protein translocation into the endoplasmic reticulum. Nature 436, 285-289.

Gorlich, D., and Rapoport, T. A. (1993). Protein translocation into proteoliposomes reconstituted from purified components of the endoplasmic reticulum membrane. Cell 75, 615-630.

Gray, D. A., Tsirigotis, M., and Woulfe, J. (2003). Ubiquitin, proteasomes, and the aging brain. Sci Aging Knowledge Environ 2003, RE6.

Hamman, B. D., Hendershot, L. M., and Johnson, A.E. (1998) BiP maintains the permeability barrier of the ER membrane by sealing the lumenal end of the translocon pore before and early in translocation. Cell 92, 747-758.

Hegde, R. S., and Lingappa, V. R. (1996). Sequence-specific alteration of the ribosome-membrane junction exposes nascent secretory proteins to the cytosol. Cell 85, 217-228.

Hegde, R. S., Mastrianni, J. A., Scott, M. R., DeFea, K. A., Tremblay, P., Torchia, M., DeArmond, S. J., Prusiner, S. B., and Lingappa, V. R. (1998a). A transmembrane form of the prion protein in neurodegenerative disease. Science 279, 827-834.

Hegde, R. S., Voigt, S., Rapoport, T. A., and Lingappa, V. R. (1998b). TRAM regulates the exposure of nascent secretory proteins to the cytosol during translocation into the endoplasmic reticulum. Cell 92, 621-631.

Kim, S. J., and Hegde, R. S. (2002). Cotranslational partitioning of nascent prion protein into multiple populations at the translocation channel. Mol Biol Cell 13, 3775-3786.

Kim, S. J., Mitra, D., Salerno, J. R., and Hegde, R. S. (2002). Signal sequences control gating of the protein translocation channel in a substrate-specific manner. Dev Cell 2, 207-217.

Levine, C. G., Mitra, D., Sharma, A., Smith, C. L., and Hegde, R. S. (2005). The Efficiency of Protein Compartmentalization into the Secretory Pathway. Mol Biol Cell.

Lu, P. D., Jousse, C., Marciniak, S. J., Zhang, Y., Novoa, I., Scheuner, D., Kaufman, R. J., Ron, D., and Harding, H. P. (2004). Cytoprotection by pre-emptive conditional phosphorylation of translation initiation factor 2. Embo J 23, 169-179.

Menetret, J. F., Hegde, R. S., Heinrich, S. U., Chandramouli, P., Ludtke, S. J., Rapoport, T. A., and Akey, C. W. (2005). Architecture of the ribosome-channel complex derived from native membranes. J Mol Biol 348, 445-457.

Nicchitta, C. V., and Blobel, G. (1993). Lumenal proteins of the mammalian endoplasmic reticulum are required to complete protein translocation. Cell 73, 989-998.

Ooi, C. E., and Weiss, J. (1992). Bidirectional movement of a nascent polypeptide across microsomal membranes reveals requirements for vectorial translocation of proteins. Cell 71, 87-96.

Ott, C. M., and Lingappa, V. R. (2004). Signal sequences influence membrane integration of the prion protein. Biochemistry 43, 11973-11982.

Rane, N. S., Yonkovich, J. L., and Hegde, R. S. (2004). Protection from cytosolic prion protein toxicity by modulation of protein translocation. EMBO J 23, 4550-4559. Epub 2004 Nov 4554.

Rutkowski, D. T., Lingappa, V. R., and Hegde, R. S. (2001). Substrate-specific regulation of the ribosome- translocon junction by N-terminal signal sequences. Proc Natl Acad Sci U S A 98, 7823-7828.

Rutkowski, D. T., Ott, C. M., Polansky, J. R., and Lingappa, V. R. (2003). Signal sequences initiate the pathway of maturation in the endoplasmic reticulum lumen. J Biol Chem 278, 30365-30372.

Scheuner, D., Mierde, D. V., Song, B., Flamez, D., Creemers, J. W., Tsukamoto, K., Ribick, M., Schuit, F. C., and Kaufman, R. J. (2005). Control of mRNA translation preserves endoplasmic reticulum function in beta cells and maintains glucose homeostasis. Nat Med 11, 757-764.

Scheuner, D., Song, B., McEwen, E., Liu, C., Laybutt, R., Gillespie, P., Saunders, T., Bonner-Weir, S., and Kaufman, R. J. (2001). Translational control is required for the unfolded protein response and in vivo glucose homeostasis. Mol Cell 7, 1165-1176.

Sciaky, N., Presley, J., Smith, C., Zaal, K. J., Cole, N., Moreira, J. E., Terasaki, M., Siggia, E., and Lippincott-Schwartz, J. (1997). Golgi tubule traffic and the effects of brefeldin A visualized in living cells. J Cell Biol 139, 1137-1155.

Stewart, R. S., and Harris, D. A. (2001). Most pathogenic mutations do not alter the membrane topology of the prion protein. J Biol Chem 276, 2212-2220.

Tan, S., Wood, M., and Maher, P. (1998). Oxidative stress induces a form of programmed cell death with characteristics of both apoptosis and necrosis in neuronal cells. J Neurochem 71, 95-105.

Turner, G. C., and Varshavsky, A. (2000). Detecting and measuring cotranslational protein degradation in vivo. Science 289, 2117-2120.

Voigt, S., Jungnickel, B., Hartmann, E., and Rapoport, T. A. (1996). Signal sequence-dependent function of the TRAM protein during early phases of protein transport across the endoplasmic reticulum membrane. J Cell Biol 134, 25-35.